The Astrophysical Journal, 838:98 (6pp), 2017 April 1 https://doi.org/10.3847/1538-4357/aa65d5

On the Magnetic Field of the Ultraluminous X-Ray Pulsar M82 X-2

Kun Xu[1] and Xiang-Dong Li[1,2]
[1] Department of Astronomy, Nanjing University, Nanjing 210023, China; lixd@nju.edu.cn
[2] Key Laboratory of Modern Astronomy and Astrophysics, Nanjing University, Ministry of Education, Nanjing 210023, China
Received 2016 November 28; revised 2017 February 15; accepted 2017 March 7; published 2017 March 30

Abstract

The discovery of the ultraluminous X-ray pulsar M82 X-2 has stimulated lively discussion on the nature of the accreting neutron star. In most of the previous studies the magnetic field of the neutron star was derived from the observed spin-up/down rates based on the standard thin, magnetized accretion disk model. However, under super-Eddington accretion the inner part of the accretion disk becomes geometrically thick. In this work we consider both radiation feedback from the neutron star and the sub-Keplerian rotation in a thick disk and calculate the magnetic moment–mass accretion rate relations for the measured rates of spin change. We find that the derived neutron star's dipole magnetic field depends on the maximum accretion rate adopted, but is likely $\lesssim 10^{13}$ G. The predicted accretion rate change can be used to test the proposed models by comparison with observations.

Key words: binaries: general – stars: neutron – X-rays: binaries

1. Introduction

M82 X-2 (or NuSTAR J095551+6940.8) is an ultraluminous X-ray source (ULX) discovered in the nuclear region of the galaxy M82 (Kaaret et al. 2006; Kong et al. 2007; Feng & Soria 2011). ULXs are very bright X-ray sources with isotropic X-ray luminosities higher than $10^{39}\,\mathrm{erg\,s^{-1}}$. They have been proposed to be stellar-mass black holes (BHs) in X-ray binaries accreting at a super-Eddington rate, and the ultrahigh luminosities may partly come from geometrical beaming in an accretion funnel (King et al. 2001; Roberts 2007). However, the 1.37 s pulsations discovered from M82 X-2 definitely result from the rotation of a magnetized neutron star (NS) rather than a BH (Bachetti et al. 2014). Its X-ray luminosity varied between 10^{39} and $10^{40}\,\mathrm{erg\,s^{-1}}$ (Brightman et al. 2016), much higher than the Eddington limit ($L_{\rm E}\sim 10^{38}\,\mathrm{erg\,s^{-1}}$, corresponding to an accretion rate of $\dot{M}_{\rm E}\sim 10^{18}\,\mathrm{g\,s^{-1}}$) for an NS with a typical mass of $1.4\,M_{\odot}$. Combining with the fact that the donor star's mass is $>5\,M_{\odot}$ (Bachetti et al. 2014), this indicates that the binary is undergoing rapid mass transfer on a thermal timescale through Roche lobe overflow (Frago et al. 2015; Shao & Li 2015). More recently, two more NS ULXs were discovered, that is, XMMU J235751.1−323725 in NGC7793 P13, with a pulse period of ∼0.42 s (Fürst et al. 2016; Israel et al. 2017b), and ULX-1 in NGC 5907, with a pulse period of ∼1.1 s (Israel et al. 2017a). The peak luminosities for these two sources are $\sim 10^{40}$ and $\sim 10^{41}\,\mathrm{erg\,s^{-1}}$, respectively, also significantly higher than the Eddington luminosity.

NS ULXs provide a unique opportunity to investigate the formation of young NSs in binaries. Obviously their dipole magnetic field strengths play a vital role in determining their nature. Besides cyclotron line feature measurements (Coburn et al. 2002; Caballero & Wilms 2012, for reviews), there are basically two (indirect) ways to estimate the *dipole* magnetic fields of NSs in X-ray binaries. One is from the rates of spin variation. The torque exerted by an accretion disk on an NS is composed by the material torque due to angular momentum transfer from the accreted matter and the magnetic torque originating from the interaction between the NS magnetic field and the disk (Ghosh & Lamb 1979), both depending on the size of the magnetosphere (Bhattacharyya & Chakrabarty 2017). The other assumes that the abrupt change in X-ray luminosity is caused by a transition between the accretion and propeller regimes, which occurs when the magnetospheric radius equals the so-called corotation radius. By these ways, the magnetic field of M82 X-2 has been estimated to range from $\lesssim 10^{9}$ to $>10^{14}$ G (Bachetti et al. 2014; Dall'Osso et al. 2015, 2016; Eksi et al. 2015; Kluźniak & Lasota 2015; Tong 2015; Christodoulou et al. 2016; Karino & Miller 2016; King & Lasota 2016; Tsygankov et al. 2016; Chen 2017).

It is noted that the above results critically depend on the inner radius of the accretion disk (or the magnetospheric radius) r_0. However, all the previous works except Dall'Osso et al. (2016) adopt the standard thin-disk model and the traditional Alfvén radius to estimate r_0, incompatible with the fact that M82 X-2 was accreting at a super-Eddington accretion rate. Recently Dall'Osso et al. (2016) considered that the dependence of r_0 on the accretion rate $\dot{M}$ changes from $r_0\propto \dot{M}^{-2/7}$ in the gas-pressure-dominated regime to $r_0\propto \dot{M}^{-1/7}$ in the radiation-pressure-dominated regime when the accretion rate is close to the Eddington limit (Ghosh 1996). We note that the r_0–$\dot{M}$ relation could be more complicated for a (super-)Eddington accreting compact star, as indicated by both observational and theoretical studies. For example, Weng & Zhang (2011) and Weng et al. (2014) investigated the disk evolution in several BH and NS X-ray binaries from low to super-Eddington luminosity and showed that the inner disk radius increases with luminosity when it becomes higher than 0.3 times the Eddington luminosity. A similar conclusion was reached by Chiang et al. (2016) in the study of the bright NS system Serpens X-1. From a theoretical point of view, Andersson et al. (2005) pointed out that radiation pressure can substantially influence the dynamics and structure of the inner region of the disk for (super-)Eddington accreting sources, which is likely to be dominated by advection rather radiative cooling (Narayan & Yi 1994).

In this paper, we consider the accretion torques in two types (i.e., thin and thick) of disk models to study the spin evolution of M82 X-2. By comparing the theoretical predictions with observations, we can constrain the NS magnetic field in each model. In particular, we show that the dependence of the spin-

up/down rate on luminosity is quite different in these models, and this may offer a useful test of the proposed models.

2. Disk Models

2.1. Thin-disk Model

Our thin-disk model is based on the original work of Ghosh & Lamb (1979) and modified by Wang (1987, 1995). In this model the NS magnetic field lines are assumed to thread the accretion disk owing to various instabilities and freeze with the disk plasma, so they become twisted and exert a torque on the NS owing to differential rotation between the NS and the disk. The inner radius of the disk is given by

$$r_0 = \xi r_{\rm A}, \tag{1}$$

where ξ is in the range of $0.5-1$ and $r_{\rm A}$ is the traditional Alfvén radius for spherical accretion

$$r_{\rm A} = \left(\frac{\mu^4}{2GM\dot{M}^2}\right)^{1/7}, \tag{2}$$

where $\mu = BR^3$ is the magnetic dipole moment, B the dipole magnetic field, M the mass, and R the radius of the NS, respectively, and G is the gravity constant. Letting the Keplerian angular velocity $\Omega_{\rm K}(r)$ at the radius r equal the angular velocity $\Omega_{\rm s}$ of the NS, one can define the corotation radius $r_{\rm c}$,

$$r_{\rm c} = \left(\frac{GM}{\Omega_{\rm s}^2}\right)^{1/3}. \tag{3}$$

If $r_0 < r_{\rm c}$, accretion can take place, and the accreted material by the NS transfers angular momentum at a rate of

$$N_0 = \dot{M}(GMr_0)^{1/2}. \tag{4}$$

Besides this (material) torque, the interaction between the twisted magnetic field lines and the disk exerts an additional torque on the NS. In the inner part of the disk with $r_0 < r < r_{\rm c}$ the disk matter rotates more rapidly than the NS, giving a spin-up torque N_+, while in the outer part with $r > r_{\rm c}$ a spin-down torque N_- is yielded. So the total torque on the NS can be written as

$$N = N_0 + N_+ + N_-. \tag{5}$$

The sum of N_0, N_+, and N_- depends on B, $\dot{M}$, and $\Omega_{\rm s}$ and can be written in the following form:

$$N = N_0 f(\omega_s), \tag{6}$$

where $f(\omega_{\rm s})$ is a function of the "fastness parameter" $\omega_{\rm s} \equiv \Omega_{\rm s}/\Omega_{\rm K}(r_0)$. Since the work of Ghosh & Lamb (1979), various forms of the function $f(\omega_s)$ have been worked out under different conditions (e.g., Wang 1987, 1995; Campbell 1997; Matt & Pudritz 2005; Dai & Li 2006; Kluźniak & Rappaport 2007; D'Angelo & Spruit 2010). Here we adopt a simplified form,

$$f(\omega_{\rm s}) = 1 - \frac{\omega_{\rm s}}{\omega_{\rm c}}, \tag{7}$$

where $\omega_{\rm c}$ is the critical fastness parameter when the net torque vanishes, ranging between 0.7 and 0.95 (Wang 1995; Li & Wang 1996). There is no essential difference between Equation (7) and the more sophisticated ones in the above-mentioned works.[3] The spin evolution of the NS is then described by

$$I\dot{\Omega}_{\rm s} = N_0\left(1 - \frac{\omega_{\rm s}}{\omega_{\rm c}}\right), \tag{8}$$

where I is the moment of inertia of the NS. After some transformation, we can rewrite Equation (8) to be

$$-\frac{a\dot{P}_{-10}}{\mu_{30}^{2/7}P^2\dot{m}^{6/7}} = 1 - \frac{b\mu_{30}^{6/7}}{P\dot{m}^{3/7}}, \tag{9}$$

where $\dot{P}_{-10}$ is the time derivative of the spin period P in units of 10^{-10} s s^{-1}, $\dot{m} = \dot{M}/\dot{M}_{\rm cr}$, $\mu_{30} = \mu/10^{30}$ G cm^3,

$$a = 1.77 \times 10^{-18}\xi^{-1/2}I(GM)^{-3/7}\dot{M}_{\rm cr}^{-6/7}, \tag{10}$$

and

$$b = 2.8 \times 10^{26}\xi^{3/2}(GM)^{-5/7}\dot{M}_{\rm cr}^{-3/7}\omega_{\rm c}^{-1}, \tag{11}$$

with $\dot{M}_{\rm cr}$ being the maximum accretion rate for an NS, which can be different from and even larger than the traditional Eddington value $\dot{M}_{\rm E}$ (see below).

2.2. Thick-disk Model

For a rapidly accreting NS, radiation inside the disk and from the NS becomes important in determining the dynamics and structure of the inner disk region. In the classic model for super-Eddington accretion a slim/thick inner disk is surrounded by an outer thin disk (Abramowicz et al. 1988; Watarai et al. 2000; Sadowski 2011). The transition radius that connects the inner and outer disks depends on the accretion rate (Yuan & Narayan 2004; Gu 2012) and is larger than the corotation radius for M82 X-2 when $L_{\rm X} > 10^{39}$ erg s^{-1} (Dall'Osso et al. 2016). This means that the traditional thin-disk model is inappropriate for M82 X-2. Two key points should be taken into account for the thick-disk model (Yi et al. 1997; Andersson et al. 2005). First, since the energy inside the inner disk is mainly transported through advection, the rotation of the disk matter becomes sub-Keplerian, that is,

$$\Omega(r) = A\Omega_{\rm K}(r), \tag{12}$$

with $A < 1$. Second, radiation pressure pushes the disk outward, and the inner disk radius is correspondingly modified. In terms of the comoving radiation flux $L_{\rm co}$, one can get the radiation pressure gradient to be (Andersson et al. 2005)

$$\frac{{\rm d}P_{\rm rad}}{{\rm d}r} = -\rho\frac{GM}{r^2}\frac{L_{\rm co}}{L_{\rm cr}}, \tag{13}$$

where ρ is the density in the disk and $L_{\rm cr}$ is the maximum luminosity corresponding to $\dot{M}_{\rm cr}$. Thus, the net gravitational force is $\left(1 - \frac{L_{\rm co}}{L_{\rm cr}}\right)\frac{GM}{r^2} = A^2\frac{GM}{r^2}$, where $A = \sqrt{1 - \frac{L_{\rm co}}{L_{\rm cr}}} = \sqrt{1-\dot{m}}$ and $\dot{m} = \dot{M}/\dot{M}_{\rm cr}$.

The sinusoidal pulse profiles observed in both M82 X-2 (Bachetti et al. 2014) and XMMU J235751.1−323725 in NGC 7793 P13 (Fürst et al. 2016) seem to suggest that radiation from the NS is nearly isotropic. However, numerical simulations

[3] Note that the original form in Ghosh & Lamb (1979), which has been used by many authors, was criticized by Wang (1987) as being inconsistent.

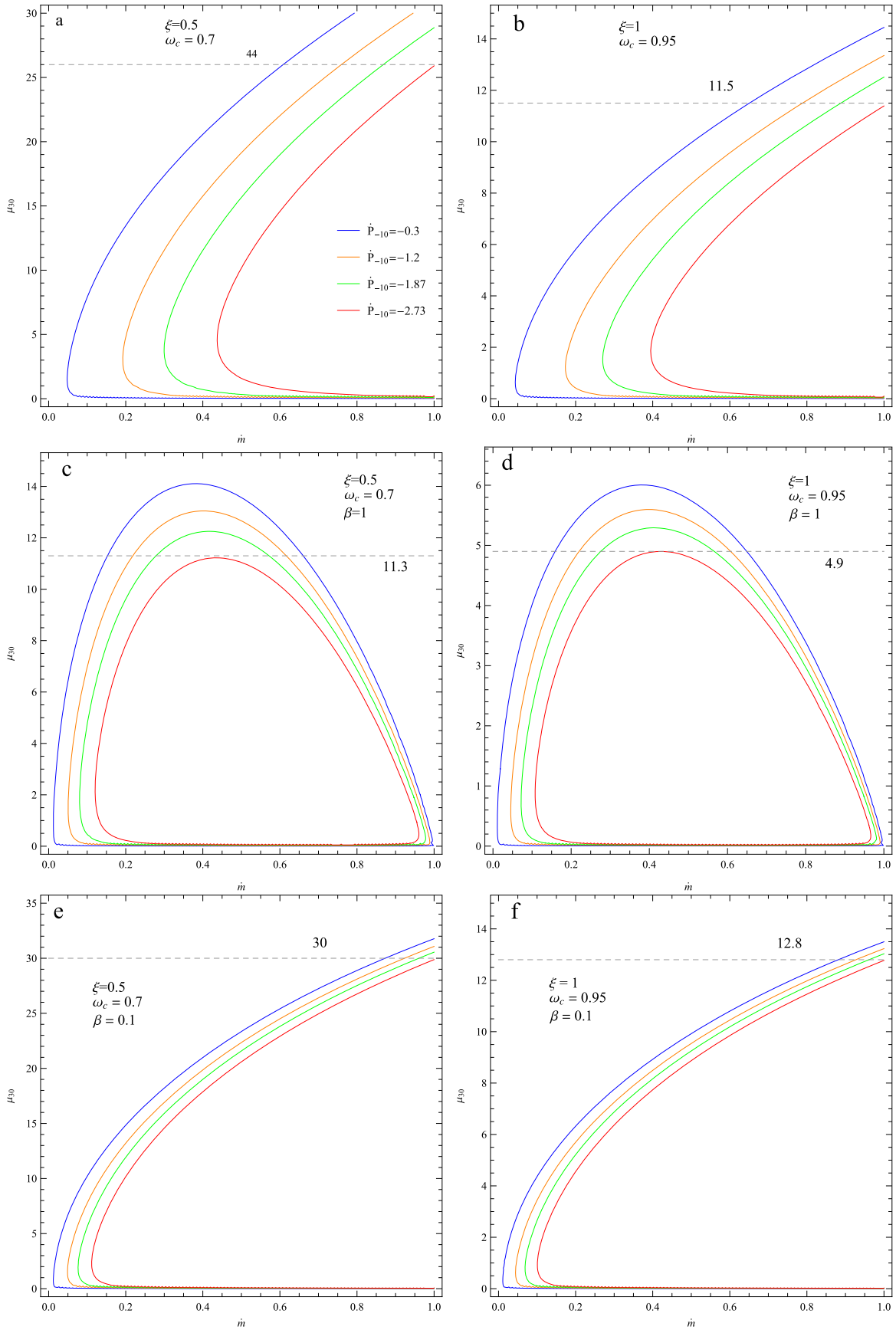

Figure 1. The μ_{30}–$\dot{m}$ relations for M82 X-2 in thin- and thick-disk models considering all four measured values of the period derivative (Bachetti et al. 2014), which are -3.0×10^{-11} (blue line), -1.2×10^{-10} (orange line), -1.87×10^{-10} (green line), and -2.73×10^{-10} (red line) (in units of s s^{-1}) at ObsID 6, 7, 8–9, and 11, respectively. The maximum accretion rate is taken to be $\dot{M}_{\rm cr} = 10^{20}$ g s^{-1}. The upper panels are for the thin-disk model, and the middle and lower panels are for the thick-disk model with $\beta = 1$ and $\beta = 0.1$, respectively. In the left and right panels we take $\xi = 0.5$, $\omega_c = 0.7$ and $\xi = 1$, $\omega_c = 0.95$, respectively.

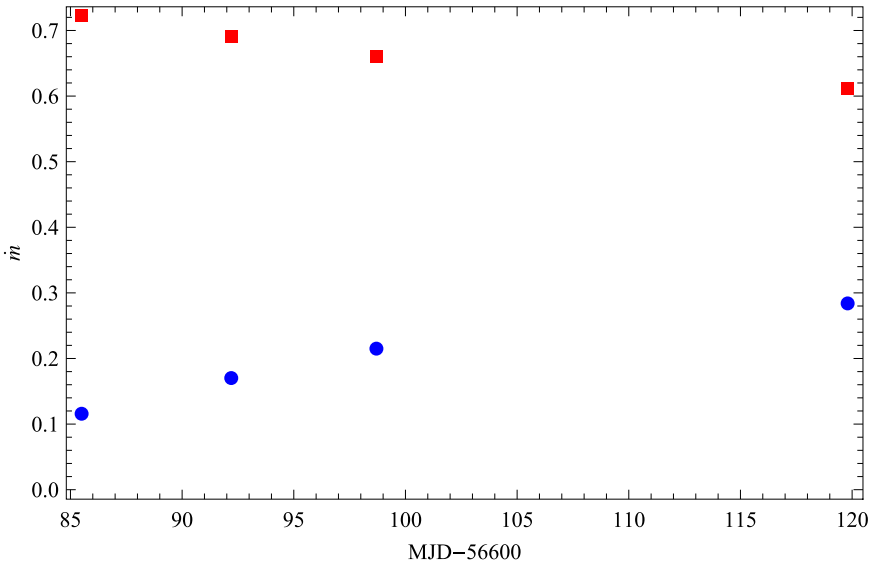

Figure 2. Predicted accretion rate at the four observational epochs with $\mu_{30} = 10$. The blue filled circles represent the solutions of the thin-disk model and the left branch solutions of the thick-disk model with $\beta = 1$, while the red filled squares represent the right branch solutions in the thick-disk model.

revealed anisotropic emission for super-Eddington accretion (e.g., Ohsuga 2007; Kawashima et al. 2016). It is unclear how smooth pulse profiles can be produced in such a case, and a possible scenario was recently discussed by Mushtukov et al. (2017). Taking into account possible beamed emission, we can write a more general form as $A = \sqrt{1 - \beta\dot{m}}$, where β (<1) is the beaming factor. We start from the derivation of the Alfvén radius in spherical accretion. The mass density is given by

$$\rho = \frac{\dot{M}}{4\pi r^2 v_{\rm r}}, \tag{14}$$

where the radial velocity $v_{\rm r} = Av_{\rm ff} = A\sqrt{2GM/r}$ owing to reduced gravitational force, and $v_{\rm ff}$ is the freefall velocity. We can estimate the modified Alfvén radius $r'_{\rm A}$ from the condition for the balance between the magnetic, radiation, and ram pressures,

$$\left.\frac{B^2}{8\pi}\right|_{r'_{\rm A}} = \rho v_{\rm r}^2|_{r'_{\rm A}} = A^2\rho v_{\rm ff}^2|_{r'_{\rm A}}. \tag{15}$$

Thus,

$$r'_{\rm A} = A^{-2/7} r_{\rm A}. \tag{16}$$

If we adopt the inner disk radius as $r'_0 = \xi r'_{\rm A}$, then we have

$$r'_0 = A^{-2/7} r_0. \tag{17}$$

Note that $r'_0 \to r_0$ when $\beta\dot{m} \ll 1$ and increases rather than decreases with $\dot{m}$ when $\beta\dot{m} \to 1$, in agreement with the observational results of luminous X-ray binaries (Weng & Zhang 2011; Weng et al. 2014; Chiang et al. 2016).

In the thick-disk model, the material torque is changed to be

$$N'_0 = A\dot{M}(GMr'_0)^{1/2} = A^{6/7}\dot{M}(GMr_0)^{1/2}, \tag{18}$$

because of sub-Keplerian rotation, and the fastness parameter is correspondingly

$$\omega'_{\rm s} = \Omega_{\rm s}/[A\Omega_{\rm K}(r'_0)]. \tag{19}$$

Similar to the previous subsection, we get the equation for the spin evolution

$$I\dot{\Omega}_{\rm s} = N'_0\left(1 - \frac{\omega'_{\rm s}}{\omega_{\rm c}}\right), \tag{20}$$

or

$$-\frac{a\dot{P}_{-10}}{A^{6/7}\mu_{30}^{2/7}P^2\dot{m}^{6/7}} = 1 - \frac{b\mu_{30}^{6/7}}{A^{10/7}P\dot{m}^{3/7}}. \tag{21}$$

3. Results

We then use Equations (9) and (21) to model the spin variations observed in M82 X-2. Before doing that, we first discuss how big $\dot{M}_{\rm cr}$ can be. For a given accretion rate $\dot{M}$, the maximum torque exerted on an accreting NS is $\dot{M}(GMr_{\rm c})^{1/2}$ when r_0 reaches its maximum value of $r_{\rm c}$. Thus, we can estimate the lower limit of the accretion rate from the observed spin-up rate, i.e.,

$$-2\pi I\dot{P}/P^2 \leqslant \dot{M}(GMr_{\rm c})^{1/2}, \tag{22}$$

or

$$\dot{M} \geqslant 3.55 \times 10^{18}\dot{P}_{-10}P^{-7/3}\ {\rm g\ s^{-1}}. \tag{23}$$

In the above calculation we have adopted $M = 1.4\,M_\odot$ and $I = 10^{45}\,{\rm g\,cm^2}$. M82 X-2 experienced a spin-up at a rate of $\dot{P} \simeq -2.7 \times 10^{-10}\,{\rm s\,s^{-1}}$ (Bachetti et al. 2014), so $\dot{M} \geqslant 4.6 \times 10^{18}\,{\rm g\ s^{-1}}$. The average and largest measured spin-up rates of ULX-1 in NGC 5907 are $-8.1 \times 10^{-10}\,{\rm s\,s^{-1}}$ and $-9.6 \times 10^{-9}\,{\rm s\,s^{-1}}$, respectively (Israel et al. 2017a), giving $\dot{M} \geqslant 1.9 \times 10^{19}\,{\rm g\ s^{-1}}$ and $1.5 \times 10^{20}\,{\rm g\ s^{-1}}$. These values imply intrinsic super-Eddington accretion, which are allowed if the accretion flow is collimated by the NS's strong magnetic field, so that radiation escapes from the sides of the column above the polar regions (Basko & Sunyaev 1976a, 1976b; Mushtukov et al. 2015). Additionally, strong magnetic fields can reduce the scattering cross section for electrons to be much below

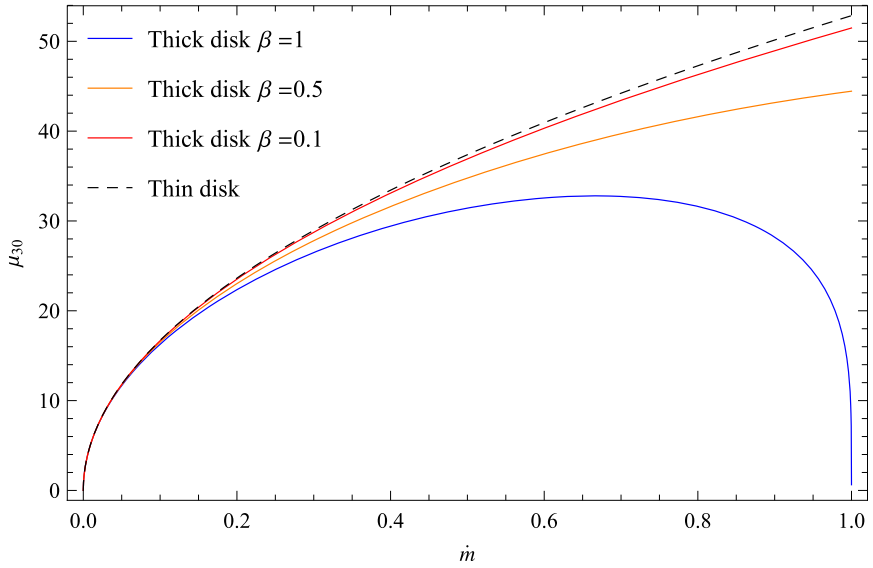

Figure 3. The μ_{30}–$\dot{m}$ relations with $\xi = 0.5$ when the inner disk radius equals the corotation radius, shown with the blue, orange, and red solid lines for the thick-disk model with $\beta = 1$, 0.5, and 0.1, respectively, and the dashed line for the thin-disk model.

the Thomson value (Canuto et al. 1971; Herold 1979; Paczynski 1992). Recently Kawashima et al. (2016) performed a two-dimensional radiation-hydrodynamic simulation of a super-Eddington accretion flow onto an NS through a channeled column and found that the total luminosity can greatly exceed $L_{\rm E}$ by several orders of magnitude.

Considering the above arguments, we first take $\dot{M}_{\rm cr} = 10^{20}$ g s^{-1}. Figure 1 presents the calculated μ_{30}–$\dot{m}$ relations for M82 X-2 in the thin- and thick-disk models, shown in the upper two and lower four panels, respectively. The four curves correspond to the four measured values of $\dot{P}_{-10}$, i.e., −0.3 (blue line), −1.2 (orange line),[4] −1.87 (green line), and −2.73 (red line) (Bachetti et al. 2014). We assume $\xi = 0.5$, $\omega_{\rm c} = 0.7$ in the left panels and $\xi = 1$, $\omega_{\rm c} = 0.95$ in the right panels. In the middle and lower panels we take $\beta = 1$ and 0.1, respectively.

In the thin-disk model (panels (a) and (b)), there can be two solutions of μ_{30} for a given $\dot{m}$, with the smaller one corresponding to $\omega_{\rm s} \ll \omega_{\rm c}$ and the larger one corresponding to $\omega_{\rm s} \sim \omega_{\rm c}$ (see also Dall'Osso et al. 2015). Only the common values of the μ_{30} for the four curves give a self-consistent estimate of μ_{30}. In panels (a) and (b) they give $\mu_{30} < 44$ and $\mu_{30} < 11.5$ for the thin disk, respectively.

In the thick-disk model with $\beta = 1$ (panels (c) and (d), with the values of ξ and $\omega_{\rm c}$ the same as in panels (a) and (b), respectively), there is one more branch of solution when $\dot{m} > \sim 0.45$, with μ_{30} decreasing with $\dot{m}$, so the μ_{30}–$\dot{m}$ curve becomes closed in the spin-up case. There are actually three branches of common μ_{30} values for the four curves. In panel (c) they are $\mu_{30} < 11.3$ for the left and right branches and $\mu_{30} \sim 2 \times 10^{-2}$ for the bottom branch; in panel (d) they are $\mu_{30} < 4.9$ for the left and right branches and $\mu_{30} \sim 7 \times 10^{-3}$ for the bottom branch.[5] When β becomes small, the solutions will recover to the thin-disk case. It can be seen that the μ_{30}–$\dot{m}$ relations in panels (e) and (f) become similar to those in the thin-disk model, and they give $\mu_{30} < 35$ and $\mu_{30} < 12.8$, respectively. The results in Figure 1 indicate that the inferred dipole field strength of M82 X-2 can be a few times smaller in the thick-disk model than in the thin-disk model, with its maximum being $\sim 1 \times 10^{13}$ G and $\sim 4 \times 10^{13}$ G, respectively.

We then change the value of $\dot{M}_{\rm cr}$ to explore its influence on the results. When $\dot{M}_{\rm cr} = 10^{19}$ g s^{-1}, the two models can only account for the period derivative $\dot{P} = -3.0 \times 10^{-11}$, so this choice is disfavored. When $\dot{M}_{\rm cr} = 10^{21}$ g s^{-1}, we get similar solutions to those in the case of $\dot{M}_{\rm cr} = 10^{20}$ g s^{-1}. The difference is that larger ranges of the dipole field are obtained. The maximum allowed μ_{30} is ∼45 in the thick-disk model with $\beta = 1$.

Figure 2 shows the predicted mass accretion rates based on the results in Figure 1 with $\mu_{30} = 10$ at the four observational epochs when X-ray pulsations were detected. The evolutionary trend of $\dot{m}$ with time can be potentially used to test which model can better reproduce the observed ones. In Figure 2 the blue filled circles represent the solutions of the thin-disk model and the left branch solutions of the thick-disk model with $\beta = 1$, and the red filled squares represent the right branch solutions of the thick-disk model with $\beta = 1$. The light curve in Figure 1 of Bachetti et al. (2014) shows that the count rate of M82 X-2 seems to slightly increase from ObsID 6 to 9, followed by a remarkable decrease toward ObsID 11. Note that the blue filled circles show a constant increase in $\dot{m}$, which is in contradiction with observations of the flux decrease. The red filled squares reveal a decrease in $\dot{m}$ at ObsID 11, but a similar trend is also seen from ObsID 6 to 9. This could be due to the fact that we have adopted a constant β in the thick-disk model. In fact, β might be inversely proportional to $\dot{m}$ (King 2009), so the flux with larger $\dot{m}$ (e.g., at ObsID 6) could be lower. However, we caution that in the 70″-radius region there are two bright sources, i.e., X-1 and X-2, as well as other fainter point sources, and it is not certain whether the observed variation in the X-ray flux was mainly contributed by X-2.

[4] In Bachetti et al. (2014) the spin-up/down rates at ObsID 7–9 are not physical values, so we use the average spin-up/down values during those intervals. We thank the referee for clarification.

[5] The bottom branch solutions are less favored but not excluded. Almost all young NSs have relatively strong ($>10^{11}$ G) magnetic fields, and low magnetic fields are generally due to extensive accretion episodes, which seem unlikely in high-mass X-ray binaries (Bhattacharya & van den Heuvel 1991).

4. Discussion

In this work we demonstrate that the observed spin variations in M82 X-2 and the other NS ULXs require that the real accretion rates of the NSs must have been super-Eddington, and in this case the thin-disk models adopted in previous works seem not self-consistent. We develop a thick-disk model by including both the radiation feedback from the accreting NS and the sub-Keplerian rotating behavior in the inner disk. We show that to account for the observed spin changes, the dipole magnetic field of M82 X-2 is less than a few $\times 10^{13}$ G, depending on the maximum accretion rate $\dot{M}_{\rm cr}$. This suggests that M82 X-2 is likely an NS with a traditional dipole field $\lesssim 10^{13}$ G.

Assuming that the propeller effect occurs at luminosity of $\sim 10^{40}$ erg s^{-1} in M82 X-2, Tsygankov et al. (2016) estimated its magnetic field to be $\sim 10^{14}$ G by equating the inner disk radius proposed by Ghosh & Lamb (1979) with the corotation radius. As we argued above, in the thick-disk case, the inner disk radius may deviate from that in the thin-disk case. A comparison of the μ–$\dot{m}$ relations for the occurrence of the propeller effect in the thin- and thick-disk models is shown in Figure 3. We can see that in the thin-disk model μ always increases with $\dot{m}$ under the condition of $r_0 = r_c$, so a high μ is inferred for a high $\dot{m}$. In the thick-disk case, μ becomes smaller for a given $\dot{m}$ with increasing β. When $\beta = 1$, μ starts to decrease with $\dot{m}$ when $\dot{m} > \sim 0.7$; thus, a very high μ may not be required. This is consistent with the current view that magnetars are very young NSs (with ages less than a few $\times 10^4$ yr), since ultrahigh fields decay by Ohm diffusion and Hall drift on a timescale $<10^5$–10^6 yr (Turolla et al. 2015, for a review). In high-mass X-ray binaries with a donor star of mass $\sim$5–10 $M_\odot$, it usually takes more than 10^7 yr (i.e., the main-sequence lifetime of the companion star) for the systems to enter the Roche lobe overflow phase after the birth of the NS (Bhattacharya & van den Heuvel 1991; Shao & Li 2015), so the NS magnetic field may have already decayed into the normal range even if it was born as a magnetar.

We are grateful to an anonymous referee for very helpful comments. This work was supported by the National Program on Key Research and Development Project (grant no. 2016YFA0400803) and the Natural Science Foundation of China under grant nos. 11133001 and 11333004.

References

Abramowicz, M. A., Czerny, B., Lasota, J.-P., & Szuszkiewicz, E. 1988, ApJ, 332, 646
Andersson, N., Glampedakis, K., Haskell, B., & Watts, A. L. 2005, MNRAS, 361, 1153
Bachetti, M., Harrison, F. A., Walton, D. J., et al. 2014, Natur, 514, 202
Basko, M. M., & Sunyaev, R. A. 1976a, MNRAS, 175, 395
Basko, M. M., & Sunyaev, R. A. 1976b, SvA, 20, 537
Begelman, M. 2002, ApJ, 568, 97
Bhattacharya, D., & van den Heuvel, E. P. J. 1991, PhR, 203, 1
Bhattacharyya, S., & Chakrabarty, D. 2017, ApJ, 835, 4
Brightman, M., Harrison, F. A., Walton, D. J., et al. 2016, ApJ, 816, 60
Caballero, I., & Wilms, J. 2012, MmSAI, 83, 230
Campbell, C. G. 1997, Magnetohydrodynamics in Binary Stars (Dordrecht: Kluwer)
Canuto, V., Lodenquai, J., & Ruderman, M. 1971, PhRvD, 3, 2303
Chen, W.-C. 2017, MNRAS, 465, L6
Chiang, C. Y., Morgan, R. A., Cackett, E. M., et al. 2016, ApJ, 831, 45
Christodoulou, D. M., Kazanas, D., & Laycock1, S. G. T. 2016, arXiv:1606.07096
Coburn, W., Heindl, W., Rothschild, R. E., et al. 2002, ApJ, 580, 394
Dai, H.-L., & Li, X.-D. 2006, A&A, 451, 581
Dall'Osso, S., Perna, R., Papitto, A., Bozzo, E., & Stella, L. 2016, MNRAS, 457, 3076
Dall'Osso, S., Perna, R., & Stella, L. 2015, MNRAS, 449, 2144
D'Angelo, C. R., & Spruit, H. C. 2010, MNRAS, 406, 1208
Eksi, K. Y., Andac, I. C., Cikintoglu, S., et al. 2015, MNRAS, 448, L40
Feng, H., Rao, F., & Kaaret, P. 2010, ApJL, 710, L137
Feng, H., & Soria, R. 2011, NewAR, 55, 166
Frago, T., Linden, T., Kalogera, V., & Sklias, P. 2015, ApJL, 802, L5
Frank, J., King, A. R., & Raine, D. J. 2002, Accretion Power in Astrophysics (3rd ed.; New York: Cambridge Univ. Press)
Fürst, F., Walton, D. J., Harrison1, F. A., et al. 2016, ApJL, 831, L14
Ghosh, P. 1996, ApJ, 459, 244
Ghosh, P., & Lamb, F. K. 1979, ApJ, 234, 296
Gu, W. M. 2012, ApJ, 753, 118
Gu, W.-M., & Lu, J.-F. 2000, ApJL, 540, L33
Herold, H. 1979, PhRvD, 19, 2868
Ibrahim, A. I., Swank, J. H., & Parke, W. 2003, ApJL, 584, L17
Israel, G. L., Belfiore, A., Stella, L., et al. 2017a, Sci, 355, 817
Israel, G. L., Papitto, A., Esposito, P., et al. 2017b, MNRAS, 466, L48
Kaaret, P., Simet, M. G., & Lang, C. C. 2006, ApJ, 646, 174
Karino, S., & Miller, J. C. 2016, arXiv:1605.05723
Kawashima, T., Mineshige, S., Ohsuga, K., & Ogawa, T. 2016, PASJ, 68, 83
King, A. R. 2009, MNRAS, 393, L41
King, A. R., Davies, M. B., Ward, M. J., Fabbiano, G., & Elvis, M. 2001, ApJL, 552, L109
King, A. R., & Lasota, J.-P. 2016, MNRAS, 458, L10
Kluźniak, W., & Lasota, J.-P. 2015, MNRAS, 448, L43
Kluźniak, W., & Rappaport, S. 2007, ApJ, 671, 1990
Kong, A. K. H., Yang, Y. J., Hsieh, P. Y., Mak, D. S. Y., & Pun, C. S. J. 2007, ApJ, 671, 349
Li, X.-D., & Wang, Z.-R. 1996, A&A, 307, L5
Matt, S., & Pudritz, R. E. 2005, ApJL, 632, L135
Mushtukov, A. A., Suleimanov, V. F., Tsygankov, S. S., & Ingram, A. 2017, MNRAS, 467, 1202
Mushtukov, A. A., Suleimanov, V. F., Tsygankov, S. S., & Poutanen, J. 2015, MNRAS, 454, 2539
Narayan, R., & Yi, I. 1994, ApJL, 428, L13
Ohsuga, K. 2007, PASJ, 59, 1033
Paczynski, B. 1992, AcA, 42, 145
Roberts, T. P. 2007, Ap&SS, 311, 203
Sadowski, A. 2011, PhD thesis, Nicolaus Copernicus Astronomical Center
Shao, Y., & Li, X.-D. 2015, ApJ, 802, 131
Tiengo, A., Esposito, P., Mereghetti, S., et al. 2013, Natur, 500, 312
Tong, H. 2015, RAA, 15, 517
Tsygankov, S. S., Mushtukov, A. A., Suleimanov, V. F., & Poutanen, J. 2016, MNRAS, 457, 1101
Turolla, R., Zane, S., & Watts, A. L. 2015, RPPh, 78, 116901
Wang, J.-M., & Zhou, Y.-Y. 1999, ApJ, 516, 420
Wang, Y.-M. 1987, A&A, 183, 257
Wang, Y.-M. 1995, ApJL, 449, L153
Watarai, K.-Y., Fukue, J., Takeuchi, M., & Mineshige, S. 2000, PASJ, 52, 133
Weng, S.-S., & Zhang, S.-N. 2011, ApJ, 739, 42
Weng, S.-S., Zhang, S.-N., & Zhao, H.-H. 2014, ApJ, 780, 147
Yi, I., Wheeler, J. C., & Vishniac, E. T. 1997, ApJL, 481, L51
Yuan, F., & Narayan, R. 2004, ApJ, 612, 724